



HAL
open science

Effect of charge fluctuation on nanoparticle heating in dusty plasma

S Prasanna, A. Michau, K. Hassouni, S Longo

► **To cite this version:**

S Prasanna, A. Michau, K. Hassouni, S Longo. Effect of charge fluctuation on nanoparticle heating in dusty plasma. *Plasma Sources Science and Technology*, 2019, 28 (3), pp.03LT03. 10.1088/1361-6595/ab094d . hal-02371770

HAL Id: hal-02371770

<https://cnrs.hal.science/hal-02371770>

Submitted on 22 Nov 2019

HAL is a multi-disciplinary open access archive for the deposit and dissemination of scientific research documents, whether they are published or not. The documents may come from teaching and research institutions in France or abroad, or from public or private research centers.

L'archive ouverte pluridisciplinaire **HAL**, est destinée au dépôt et à la diffusion de documents scientifiques de niveau recherche, publiés ou non, émanant des établissements d'enseignement et de recherche français ou étrangers, des laboratoires publics ou privés.

Effect of charge fluctuation on nanoparticle heating in dusty plasma

S Prasanna, A Michau, and K Hassouni

*Laboratoire des Sciences des Procédés et des Matériaux, UPR3407, CNRS,
Universite Paris 13, avenue Jean-Baptiste Clément, 93430 Villetaneuse (France)*

S Longo

Chemistry Department, Università degli Studi "Aldo Moro" di Bari, Via Orabona, 4 70126 Bari

A physically consistent discrete statistical theory for charge and temperature fluctuations is developed which is capable of determining the mean and statistical properties of particle charge and temperature distributions. The statistical parameters obtained using this model are in very good agreement with Monte-Carlo simulations. Results show that the correlation between charge and temperature fluctuations significantly affect the thermal balance for nm-sized particles. We also showed that temperature distribution of nm-sized particles have a significantly populated tail towards high temperatures which may have important consequences on the structure of the particle.

Non-thermal plasma sources have been demonstrated to be promising to produce a wide range of high quality nanoparticles (NPs) [1–3] such as nanodiamonds[4], carbon NPs [5], silicon crystals[6] and others. However, there is still lack of significant knowledge of the process of NP formation and dynamics in the plasma which is critical to produce NPs of desired size, crystallinity and quality. Nevertheless it is understood that intense heating of NPs due to electron/ion collection has an important role to determine the crystalline nature of NPs formed in the plasma [7, 8].

Several independent studies have pointed out that the particle temperatures can be significantly higher than the gas temperatures in non-equilibrium discharges [9–11]. The experiments of Arnas and Mouberti [10] on sputtering discharges, produced two distinct structures namely graphite like structures for particles of few nanometer size and amorphous carbon structures for larger particles. The structure of the NPs strongly depends on the heating of the particles. Small size particles experience intense heating to very high temperatures favoring phase transformations, where as large particles are very much in equilibrium with the gas. Mangolini and Kortshagen [7] showed using Monte-Carlo simulations that the particle temperatures can significantly fluctuate. The instantaneous temperatures of NPs can be higher than gas temperature by several hundreds of kelvins. They represented the statistics of temperature fluctuations in terms of temperature distribution functions and discussed the effects of plasma conditions and particle size on the particle temperature distribution function. It is generally found that particles of few nanometers ($d < 10 \text{ nm}$) had a very wide distribution while larger particles displayed very narrow temperature distribution.

The knowledge of a detailed energy balance of NPs in a dusty plasma is highly desirable in order to monitor the equilibrium particle temperature in the process and thereby gain finer control over the structure of the NPs produced. There is however a lack of theory that makes it possible to have a quick estimate of peak and average temperature values. In the present letter, we de-

scribe a theory of heating of an isolated nanoparticle in a dusty non-thermal plasma that take into account the correlation between stochastic charge and temperature fluctuations of the particle.

We start with the transient energy balance of the particle that can be written as

$$\frac{dT_p}{dt} = (H - L) \underbrace{\frac{S_p}{m_p C_p}}_{\alpha} \quad (1)$$

where m_p , S_p , C_p and T_p are the mass, surface area, thermal heat capacity and temperature of the particle, H and L are the heating and cooling flux experienced by the particle. For a spherical particle of radius r_p and density ρ_p , $\alpha = \frac{3}{\rho_p C_p r_p}$. As the particles are very small, the temperature of the particle can be assumed to be lumped i.e. spatially homogeneous. The nanoparticles in the plasma experience heating mainly due to bombardment of electron and ions as well as recombination of ions on the surface of the particle. In addition to this, depending on the plasma environment, particles can undergo complex surface reactions and phase transition processes with consequences on thermal balance. In the present letter, for the sake of simplicity, we restrict to dusty plasma with noble gases such as argon. So, the heating fluxes are essentially due to the collision of the particles with ions and electrons which may be expressed as:

$$H_q = \underbrace{2k_b T_e j_{e,q}}_{J_{e,q}} + \underbrace{(E_{ion} + e|\phi|) j_{i,q}}_{J_{i,q}} \quad (2)$$

where q is the instantaneous charge of the particle, $j_{e,q}$ and $j_{i,q}$ are the electron and ion flux to the particle surface, T_e is the electron temperature and, E_{ion} and ϕ are the ion recombination energy and electric potential of the particle. $2k_b T_e$ is the average energy flux of electrons that arrive at the surface of particle when the electrons follow a Maxwellian distribution at electron temperature T_e [9]. We assume OML theory to be valid for the calculation of electron and ion flux. As the particles in a

dusty plasma undergo charge fluctuations [12, 13] due to collisions with electrons and ions, the heating flux is a stochastic term and a time averaged heating flux \overline{H} has to be used to determine the average temperature T_p .

On the other hand, the main mode of cooling is through collision of particles with gas molecules (conduction). Radiation flux is generally small for the particle sizes encountered in plasma processing and can be neglected. The conduction losses to the background gas can be evaluated using Knudsen's model which takes into account the energy lost due to collisions between particles and neutral gas. This can be written as

$$L = \frac{3}{8} n_g \sqrt{\frac{8k_b T_g}{\pi m_g}} k_b (T_p - T_g) = h_c \theta_p \quad (3)$$

where n_g , m_g are the number density and mass of neutral gas species respectively and h_c is the heat transfer coefficient for the conduction process and $\theta_p = T_p - T_g$.

For stationary conditions, the average particle temperature $\overline{\theta}_p$ is $\frac{\overline{H}}{h_c}$. As a common practice, \overline{H} is approximated by $H_{q_{ref}}$ where q_{ref} is determined such that ion and electron currents to the particle are balanced i.e. $j_{e,q_{ref}} = j_{i,q_{ref}}$ [9–11]. In fact, assuming continuous statistical description of charging, Matsoukas and Russel [13] showed that the charge distribution of the particle is well represented by a Gaussian profile with a mean value equal to q_{ref} .

However, the validity of this assertion can only be tested by performing a monte carlo simulation of particle charging and heating which have been performed for the experimental conditions of Arnas and Moubéri [10]. The simulation procedure is similar to that described by Mangolini and Kortshagen [7] and can capture the statistical and transient history of charge and temperature of the particle. The frequency of electron/ion collisions is much smaller compared to collisions with neutral gas and hence electron/ion collisions are considered to be discrete and stochastic while gas cooling is considered as continuous process. Figure 1(a) shows the transient thermal history, (b) the temperature distribution function and (c) the charge distribution for carbon particles of different sizes in an Argon plasma at a pressure of 60 Pa and electron and ion concentrations $N_e = N_i = 10^{17} m^{-3}$, $T_g = 373 K$ and $T_e = 1.0 eV$. It clearly appears that small particles show much larger temperature fluctuations and larger distributions compared to the larger particles. This is because they possess lower thermal mass. Indeed these temperature fluctuations can be critical in determining the phase of the nanoparticles. Also, the small particles have narrow charge distributions (2-3 charge bins) compared to the large particles which means that the discrete nature of charge distribution significantly outweighs the Gaussian distribution approximation for charge of small particles. The average charge and temperatures based on classical averaging and monte-carlo simulations are given in Table I. It is seen that the time averaged temperatures based on q_{ref} , $\theta_p(q_{ref})$

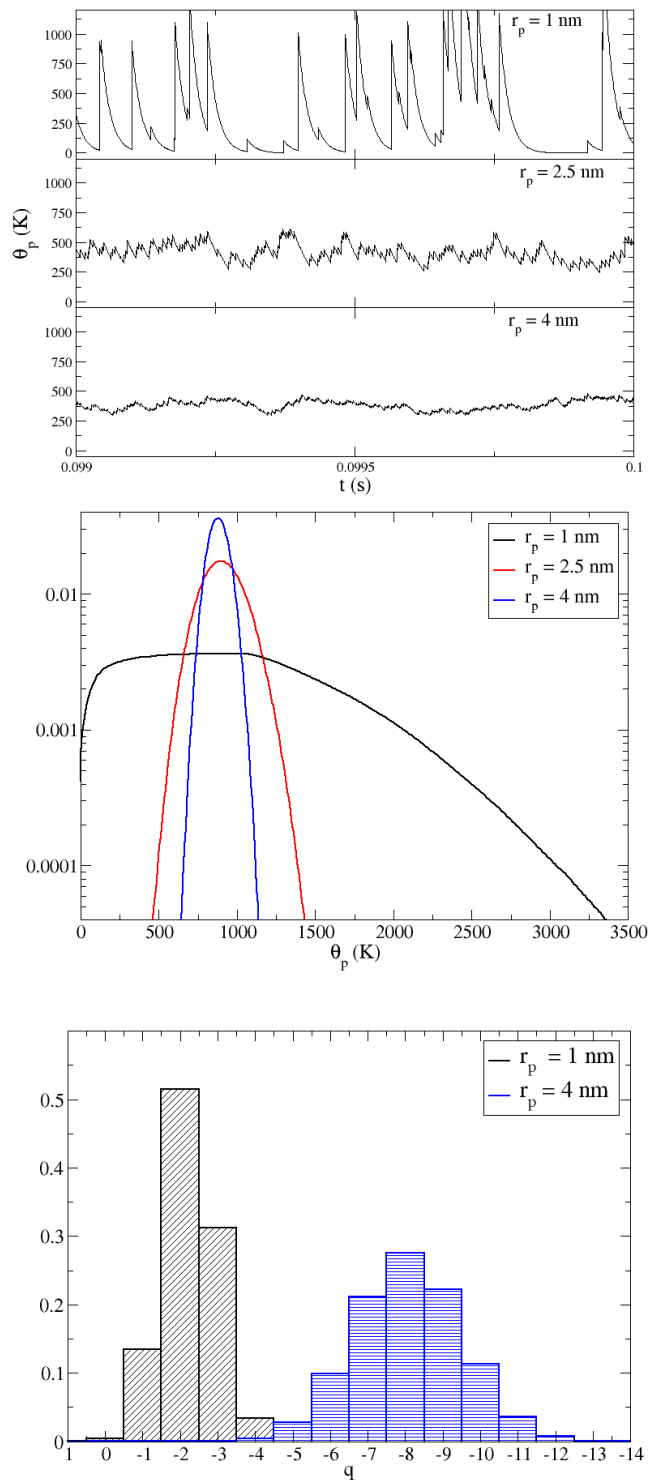


FIG. 1: (a) Transient time fluctuation, (b) temperature distribution and (c) charge distribution obtained using MC simulations for different sizes of carbon particle in an Argon plasma (experimental conditions of Arnas and Moubéri [10]) at $p = 60$ pa and $N_e = N_i = 10^{17} m^{-3}$, $T_g = 373 K$ and $T_e = 1.0 eV$.

TABLE I: The comparison between classical and Monte-carlo average charge, and time averaged temperature $\bar{\theta}_p(q_{ref})$ and average temperature from MC simulations $\bar{\theta}_{pMC}$, and the ratio of heat flux $\frac{H_{qref}}{\bar{H}_{MC}}$ where \bar{H}_{MC} is the time averaged heating flux from MC calculations. Also indicated is the standard deviation of MC average temperature obtained over 10 samples.

R_p nm	T_e (eV)	q_{ref}	\bar{q}_{MC}	$\bar{\theta}_p$ (K)	$\frac{H_{qref}}{\bar{H}_{MC}}$
				q_{ref} MC	
1 nm	0.75	-1.5	-1.8	622 797 \pm 3	0.80
	1	-2	-2.2	843 1027 \pm 2	0.84
	2	-3.6	-3.8	1847 2093 \pm 3	0.90
	3	-5	-5.3	3023 3297 \pm 4	0.93
4 nm	0.75	-6.1	-6.4	663 661 \pm 1	0.95
	1	-7.8	-8.1	842 886 \pm 2	0.96
	2	-14.2	-14.5	1838 1900 \pm 2	0.97
	3	-20.1	-20.4	2954 3016 \pm 3	0.98

are substantially lower than MC based averaged temperatures $\bar{\theta}_{pMC}$ for small particles. The difference could be as high as 120 K for particle with $r_p = 1$ nm and becomes negligible for large particles at $T_e = 1$ eV. The error in particle temperature is due to the underestimation of the average heating flux by up to 20% as seen in the table I. Simulations have also been performed to check the effects of radiative cooling on particle temperature. It is seen for most conditions, radiative cooling is insignificant with maximum change in temperature of 100 K. Also, some conditions exhibit very high particle temperatures of 3000 K which can lead to thermionic emission of electrons. However, for the plasma conditions, it is found that thermionic current are far lower than that of ion-electron currents and hence thermionic emission need not be considered for these conditions.

On closer inspection, one can write the temporal equation for the error in particle temperature $\Delta\theta_p = \bar{\theta}_{pMC} - \bar{\theta}_p(q_{ref})$, as

$$\frac{d\Delta\theta_p}{dt} = \alpha\{\bar{H} - H_{qref} - h_c\Delta\theta_p\} \quad (4)$$

where \bar{H} is the time averaged heating flux. Although the charging process is discrete in nature, for the sake of understanding the interaction between charging and thermal balance, analysis of equation 4 is first conducted assuming the charge to be continuous and for stationary conditions. Thus neglecting the higher order terms, $\Delta\theta_p$ can be approximated as

$$\Delta\theta_p \approx \frac{1}{h_c} \frac{d^2 H_{qref}}{dq^2} \sigma_q^2 \quad (5)$$

where σ_q is the standard deviation of the particle charge distribution. Using OML theory for charging and the expressions for σ_q provided by Matsoukas and Russel [13] for Gaussian charge distributions, it can be shown that $\Delta\theta_p$ is proportional to $1/r_p^2$ and T_e . This is consistent

with Figure 2 where the variation of $\Delta\theta_p$ as a function of T_e and r_p as estimated using equation 5 is shown. This shows that $\Delta\theta_p$ is small and H_{qref} is a good approximation of \bar{H} for a large particle. On the opposite, $\Delta\theta_p$ is significant for small particles thus indicating strong correlations between charge and temperature fluctuations. As a result \bar{H} cannot be approximated with H_{qref} in this case.

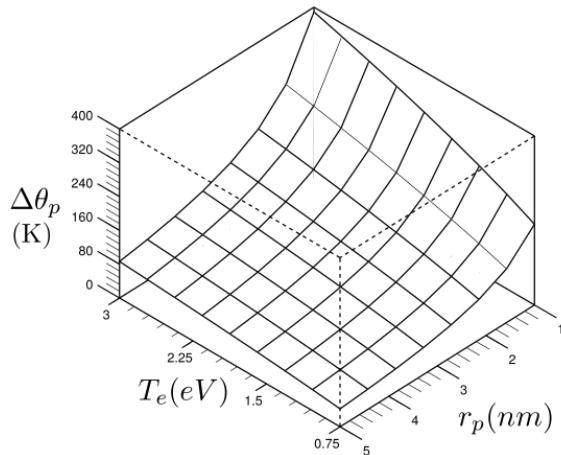


FIG. 2: Contour plot showing the variation of $\Delta\theta_p$ calculated using equation 5 as a function of T_e and r_p for the same conditions as Figure 1

Indeed, it is desirable to go beyond the continuous statistical description for charge fluctuations and develop a general theory taking into account the discrete nature of the charging and the correlation between charge and thermal fluctuations. The basic equations for charge and particle temperature can be derived from first principles using the stochastic equations for charge and temperature distribution functions f_{q,θ_p} where $\sum_q \left[\int_{\theta_p} f_{q,\theta_p} d\theta_p \right] = 1$. The main assumption here is that there is no temporal change in the particle size distribution. Due to the nature of the thermal transfer with background cold gas, the governing equations for particle temperature are expressed in terms of θ_p . The population balance equation for charge q and temperature θ_p is

$$\begin{aligned} \frac{\partial f_{q,\theta_p}}{\partial t} = & j_{e,q+1} f_{q+1,\theta'_p} S_p + j_{i,q-1} f_{q-1,\theta''_p} S_p - \\ & (j_{e,q} + j_{i,q}) f_{q,\theta_p} S_p + \frac{\partial}{\partial \theta_p} (\alpha h_c f_{q,\theta_p} \theta_p) \quad (6) \end{aligned}$$

The first four terms correspond to the ion-electron collection where the first two indicates the gain term from neighboring charge states and the next two indicates the loss terms. The last term of the equation refers to the cooling. It has to be noted that the particles entering from neighboring charge states see an *instantaneous* increase in temperature due to ion or electron collisions. In other words, $\theta'_p = \theta_p - \Delta\theta_e$ and $\theta''_p = \theta_p - \Delta\theta_i$ where

$$\Delta\theta_e = \frac{2k_b T_e}{m_p C_p} \text{ and } \Delta\theta_i = \frac{1}{m_p C_p} (E_{ion} + e|\phi|).$$

The zeroth moment of f_{q,θ_p} gives the charge distribution at q , $\psi_q = \int f_{q,\theta_p} d\theta_p$ and taking the zeroth moment of the population equation leads to the master equation of charge which is

$$\frac{1}{S_p} \frac{d\psi_q}{dt} = j_{e,q+1}\psi_{q+1} + j_{i,q-1}\psi_{q-1} - (j_{e,q} + j_{i,q})\psi_q \quad (7)$$

As it is assumed that the temperature has no effect on the charging of the particle, the cooling term does not affect the charge transfer. As the particle charging is a Poisson process, the stationary charge distribution can be obtained by applying the recursive relation between two consecutive charge states $j_{i,q}\psi_q = j_{e,q+1}\psi_{q+1}$ combined with $\sum_q \psi_q = 1$. We showed that the charge distribution thus obtained is same as the time averaged distribution calculated using monte-carlo simulations depicted in Fig. 1.

Similarly, the first moment of the population equation would lead to the average temperature of a given charge state q , $\psi_q \overline{\theta_{p,q}} = \int \theta_p f_{q,\theta_p} d\theta_p$ which is

$$\begin{aligned} \frac{1}{\alpha} \frac{d\psi_q \overline{\theta_{p,q}}}{dt} = & j_{e,q+1}\psi_{q+1}(\Delta\theta_{e,q+1} + \overline{\theta_{p,q+1}}) \\ & + (j_{i,q-1}\psi_{q-1}(\Delta\theta_{i,q-1} + \overline{\theta_{p,q-1}}) \\ & - (j_{e,q} + j_{i,q} + h_c)\psi_q \overline{\theta_{p,q}} \end{aligned} \quad (8)$$

One can identify 3 groups of source terms in Equation 8 namely the heat flux due to the attachment of electron and ion from the neighboring charge states and heat loss due to electron, ion attachment and cooling of the charge state q . The equation assumes a tridiagonal form in q and $\overline{\theta_{p,q}}$ can be determined by choosing a sufficiently wide band covering all possible charge states. Subsequently, the total average particle temperature would be $\overline{\theta_p} = \sum_q \psi_q \overline{\theta_{p,q}}$. Also, the total energy equation is the sum of all individual state equations (Eqn. 8) which becomes

$$\frac{1}{\alpha} \frac{d\overline{\theta_p}}{dt} = \sum_q \psi_q \underbrace{\{J_{e,q} + J_{i,q}\}}_{H_q} - h_c \sum_q \psi_q \overline{\theta_{p,q}} \quad (9)$$

It is to be noted that the exchange terms of sensible heat between different charge states in Equation 8 gets canceled out in the energy equation. The resulting equation is also physically consistent as the total heat flux to the particle is the sum of all heat flux at different charge states, $\overline{H} = \sum_q H_q \psi_q$. Thus one can finally obtain the expression for stationary particle temperature that takes into account charge correlation effects as

$$\overline{\theta_p} = \sum_q \psi_q \overline{\theta_{p,q}} = \frac{\sum_q H_q \psi_q}{h_c} = \frac{\overline{H}}{h_c} \quad (10)$$

In table II, we report the values of $\overline{\theta_p}$ obtained from Eqn. 10 and MC simulations for the earlier stated discharge conditions. It is seen that the two temperatures are in

TABLE II: The time-averaged temperature obtained using eqn. 10 and MC for the conditions specified in Figure 1 as a function of T_e and particle radius. Also reported are the relative difference between theoretical estimation and MC statistical quantities namely standard deviation σ_{θ_p} , skew γ_{θ_p} and kurtosis ν_{θ_p}

r_p nm	T_e eV	$\overline{\theta_p}$		Relative difference		
		MC	Eqn 10	σ_{θ_p}	γ_{θ_p}	ν_{θ_p}
1 nm	0.75	796	772	-0.014	0.02	0.008
	1.00	1031	1002	-0.011	0.023	0.006
	2.00	2093	2046	-0.013	0.003	-0.004
	3.00	3297	3254	-0.012	0.03	0.007
4 nm	0.75	663	657	0.002	0.041	0.008
	1.00	886	880	-0.001	0.013	0.004
	2.00	1900	1885	0.003	-0.005	0.013
	3.00	3016	3005	0.002	-0.03	0.004

excellent agreement within 2% relative differences. The developed theory provides therefore an accurate representation of energy balance of nm-sized particles.

The nature of the population equations enables recursive determination of moment equations of any order n , $\psi_q \overline{\theta_{p,q}^n} = \int \theta_p^n f_{q,\theta_p} d\theta_p$. In general, the n^{th} moment of the population equation is of the form

$$\begin{aligned} \frac{1}{\alpha} \frac{d\psi_q \overline{\theta_{p,q}^n}}{dt} = & j_{e,q+1}\psi_{q+1} \overline{\theta_{p,q+1}^n} + j_{i,q-1}\psi_{q-1} \overline{\theta_{p,q-1}^n} \\ & - \{j_{e,q} + j_{i,q} + nh_c\} \psi_q \overline{\theta_{p,q}^n} \\ & + j_{e,q+1}\psi_{q+1} \sum_{j=0}^{n-1} {}^n C_j \Delta\theta_{e,q+1}^{n-j} \overline{\theta_{p,q+1}^j} \\ & + j_{i,q-1}\psi_{q-1} \sum_{j=1}^n {}^n C_j \Delta\theta_{i,q-1}^{n-j} \overline{\theta_{p,q-1}^j} \end{aligned} \quad (11)$$

The nature of the above equation assumes a tridiagonal form in q and can be resolved in the same way as that for $\overline{\theta_{p,q}}$. Again, the total average moments of temperature is determined as $\overline{\theta_p^n} = \sum_q \psi_q \overline{\theta_{p,q}^n}$. For stationary conditions, the total average n^{th} moment assumes the form

$$\overline{\theta_p^n} = \frac{\sum_q \sum_{j=0}^{n-1} {}^n C_j \psi_q \overline{\theta_{p,q}^j} (j_{e,q} \Delta\theta_{e,q}^{n-j} + j_{i,q} \Delta\theta_{i,q}^{n-j})}{nh_c} \quad (12)$$

Further, calculation of higher order moments makes it possible to determine the statistical parameters such as standard deviation σ_{θ_p} , skewness γ_{θ_p} and kurtosis ν_{θ_p} , from which one can construct the temperature distribution function [14, 15]. As reported in table II, the relative differences between the statistical parameters calculated using the theory and monte-carlo simulations remains below 5%. Figure 3 shows complementary cumulative distribution functions obtained using Box-Cox power exponential distribution fit [15] from the statistical parameters of Table II. Also depicted are cumulative distribution functions obtained from MC simulations. The

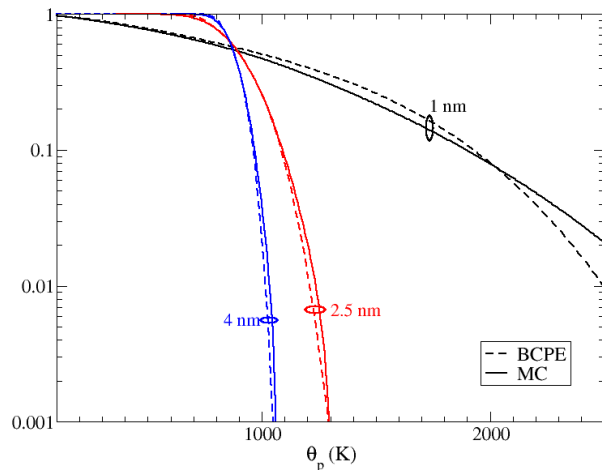


FIG. 3: Complementary cumulative temperature distribution function for particles at $T_e = 1$ eV from MC simulations and Box-Cox power exponential fit (BCPE).

comparison between the theoretical and simulated profile is satisfactory, which shows that the developed theory is capable of predicting the temperature distribution over wide range of particle sizes.

The development is useful to determine the fraction of particles above phase transition temperatures and this

can be interesting for crystalline nanoparticle synthesis. For example, the particle size of $r_p = 1$ nm has about 50% of the particle having more than 1000 K and 10% above 2000 K while only 10% of particles of size $r_p = 4$ nm are more than 1000 K at any given instant of time. Moreover, smaller particles are found to have lower phase transition temperatures[16]. This further validates the assertion that small particles can achieve crystallization more easily than larger particles in cold plasmas. In the present development, we assumed the particle size is stationary. However, in practical dusty plasma processes, the particles are continuously evolving through aerosol dynamics process. The nm-sized particles can be quickly consumed through molecular growth and inter-particle coagulation. Therefore, the overheating effect predicted by the model is effective only when the lifespan of the smallest particle before they undergo growth is much greater than the ion-electron collection characteristic time. For the processing plasma condition considered in this study, the lifespan of the particle in the 1-3 nm size is in the minute timescale [17], which translates to several charging cycles. This means that the overheating predicted by the model discussed here is likely to take place resulting in high-crystallinity for nm-sized particles. This is in full agreement with the observation made by Arnas and Moubéri [10]. The present model can be further extended to include radiative cooling for high particle temperatures and charging mechanisms such as thermoionic emission.

-
- [1] Davide Mariotti and R Mohan Sankaran. Microplasmas for nanomaterials synthesis. *Journal of Physics D: Applied Physics*, 43(32):323001, 2010.
 - [2] Kostya Ken Ostrikov, Uros Cvelbar, and Anthony B Murphy. Plasma nanoscience: setting directions, tackling grand challenges. *Journal of Physics D: Applied Physics*, 44(17):174001, 2011.
 - [3] Uwe R Kortshagen, R Mohan Sankaran, Rui N Pereira, Steven L Girshick, Jeslin J Wu, and Eray S Aydil. Non-thermal plasma synthesis of nanocrystals: fundamental principles, materials, and applications. *Chem. Rev.*, 116(18):11061–11127, 2016.
 - [4] Ajay Kumar, Pin Ann Lin, Albert Xue, Boyi Hao, Yoke Khin Yap, and R Mohan Sankaran. Formation of nanodiamonds at near-ambient conditions via microplasma dissociation of ethanol vapour. *Nature communications*, 4:2618, 2013.
 - [5] Austin Woodard, Kamran Shojaei, Giorgio Nava, and Lorenzo Mangolini. Graphitization of carbon particles in a non-thermal plasma reactor. *Plasma Chemistry and Plasma Processing*, pages 1–12, 2018.
 - [6] NJ Kramer, RJ Anthony, Meenakshi Mamunuru, ES Aydil, and UR Kortshagen. Plasma-induced crystallization of silicon nanoparticles. *Journal of Physics D: Applied Physics*, 47(7):075202, 2014.
 - [7] Lorenzo Mangolini and Uwe Kortshagen. Selective nanoparticle heating: another form of nonequilibrium in dusty plasmas. *Physical review E*, 79(2):026405, 2009.
 - [8] NJ Kramer, ES Aydil, and UR Kortshagen. Requirements for plasma synthesis of nanocrystals at atmospheric pressures. *Journal of Physics D: Applied Physics*, 48(3):035205, 2015.
 - [9] GHM Swinkels, H Kersten, H Deutsch, and GMW Kroesen. Microcalorimetry of dust particles in a radio-frequency plasma. *Journal of Applied Physics*, 88(4):1747–1755, 2000.
 - [10] C. Arnas and A. A. Moubéri. Thermal balance of carbon nanoparticles in sputtering discharges. *Journal of Applied Physics*, 105(6):1–5, 2009.
 - [11] H R Maurer and H Kersten. On the heating of nano- and microparticles in process plasmas. *Journal of Physics D: Applied Physics*, 44(17):174029, 2011.
 - [12] J Goree. Charging of particles in a plasma. *Plasma Sources Science and Technology*, 3(3):400–406, 1999.
 - [13] Themis Matsoukas and Marc Russell. Particle charging in low-pressure plasmas. *Journal of applied physics*, 77(9):4285–4292, 1995.
 - [14] Edmund A Cornish and Ronald A Fisher. Moments and cumulants in the specification of distributions. *Revue de l'Institut international de Statistique*, pages 307–320, 1938.
 - [15] Robert A Rigby and D Mikis Stasinopoulos. Smooth centile curves for skew and kurtotic data modelled using the box-cox power exponential distribution. *Statistics in medicine*, 23(19):3053–3076, 2004.
 - [16] Makoto Hirasawa, Takaaki Orii, and Takafumi Seto. Size-

- dependent crystallization of si nanoparticles. Applied physics letters, 88(9):093119, 2006.
- [17] A Michau, C Arnas, and K Hassouni. Aerosol dynamics in a sputtering dc discharge. Journal of Applied Physics, 121(16):163301, 2017.